The Meteorological Magazine

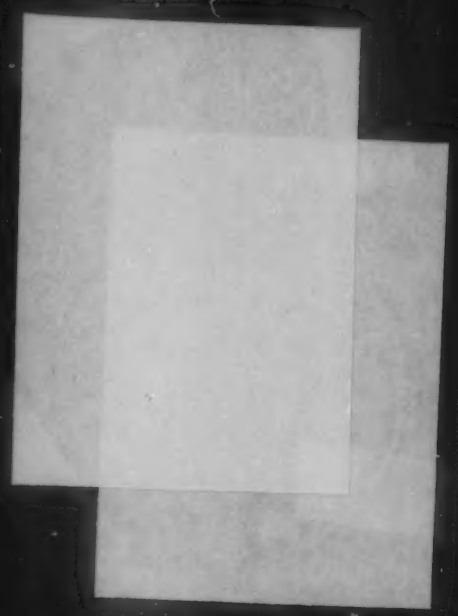

The Meteorological Magazine

March 1989
Vol. 118 No. 1400

551.577.33(41-4)

Periodic variations in extreme hourly rainfalls in the United Kingdom

B.R. May and T.J. Hitch
Meteorological Office, Bracknell

Summary

Extreme 1-hour rainfalls observed in the United Kingdom during the period 1881 to 1986 are shown to have roughly sine-wave variations with approximate periods of 7, 11, 20 and 50 years and amplitudes of 7%, 10%, 5% and 7%. The 11-year period variation and solar activity, as measured by sunspot number, have maxima and minima which are closely synchronized.

1. Introduction

This article concerns the behaviour of annual maximum 1-hour rainfalls observed at many locations in the United Kingdom during the period 1881 to 1986. The results were obtained from an analysis of these rainfalls during a comparison of their frequencies of occurrence over a long period against the frequencies recommended in the Flood Studies Report, Volume II (NERC 1975) which were based on observations over a shorter period, from 1951 to 1970. The investigation was prompted by an intriguing graph in the Flood Studies Report which showed evidence for a small, but clear periodic variation in annual maximum rainfalls for 2-hour durations in the 20-year interval.

2. The data processing

The observations used here are annual maximum rainfalls for 1-hour duration collected from all known sources and which are available in the Meteorological Office data archives. They total 4532 values with a wide range of record lengths up to 94 years, from 234 stations distributed over the whole of the United Kingdom but mainly in southern and central England.

A variation of annual maximum rainfalls which has, at a particular time, the same phase over the whole of a region can easily be hidden by the large random variations of these maxima from one year to the next observed at a particular location. A synchronous variation like this can be isolated by dividing the sequence of maxima at each station by their mean value and then, for each year, finding the median, D, of these normalized maxima from a representative selection of stations. For a region covering the whole of the United Kingdom, i.e. using all available stations' data, the D values for 1-hour rainfalls have been calculated for each year from 1881 to 1986.

3. Results

The spectrum of D (Fig. 1) shows the amplitude of components as a function of frequency at intervals of 0.01 cycles year^{-1}, along with their period in years. D has four main components with periods estimated to be within the ranges 6.9 to 7.4, 10.5 to 11.8, 18.2 to 22.2 and 40.0 to 66.7 years, defined by the 0.01 cycles year^{-1} frequency bands in Fig. 1, with corresponding amplitudes in the ratio 3:4:2:3. From the analysis described in the following sections we show that the periods are close to 7.2, 10.8, 20.0 and 50.0 years but, for simplicity, we refer to the 7-, 11-, 20- and 50-year period waves.

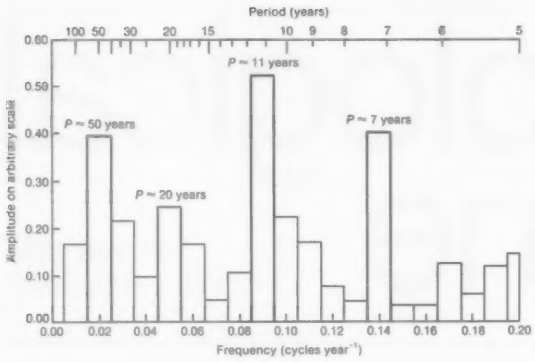

Figure 1. Frequency spectrum of D, the median normalized annual maximum 1-hour rainfall for the United Kingdom from 1881 to 1986, showing spectral components at a resolution of 0.01 cycles year^{-1}. The largest components have periods close to 7, 11, 20 and 50 years.

To remove obscuring short-period variations in D, running means over three years, D_3, have been calculated, where the means are ascribed to the middle year. D_3 is plotted against year in Fig. 2 which shows the combined effect of the four components producing near-regular episodes of maxima and minima superimposed on a longer period background variation. The numbers of normalized annual maxima contributing to the D values for each year are indicated at the top of Fig. 2 at five-year intervals.

The spectrum reveals only the periods of components but not their waveform or when their maxima and minima occur. To isolate waveforms, sliding means over selected durations can be used to suppress some components and not others. A sliding mean of duration p applied to a sine wave of period P and unit amplitude is a sine wave of amplitude $f = \sin(\pi.p/P)/(p/P)$. If f is positive the sliding-mean wave is in phase with the original wave and 180° out of phase if f is negative. If p is an exact multiple of P then $f = 0$. Although these results are true for sine waves they also hold adequately for waveforms which are approximately like sine waves in shape.

3.1 50-year period wave

This is isolated by taking running means of D over 21 years (D_{21}), which is nearly an exact multiple of 7.2, 10.8 and 20.0 years, for which f has values of +0.03, −0.03 and −0.04, so almost completely eliminating the contribution of these components. The waveform is shown by D_{21} in Fig. 3(a). It has maxima in about 1893 and 1940 and a minimum in 1915 which are consistent with a period near 50.0 years. Allowing for the reduction by smoothing over 21 years ($f = 0.73$) the mean amplitude over the whole 87-year interval is estimated to be about 7%, decreasing after 1930 to near zero from 1960 onwards.

3.2 20-year period wave

This is isolated by taking means of D over 9 years (D_9) which reduces considerably the amplitude of the 7- and 11-year period components, by factors $f = -0.18$ and +0.19, but reduces the 20- and 50-year components by smaller amounts, with $f = 0.70$ and 0.95. D_9 is plotted in Fig. 3(a) in which the 20-year wave is seen to modulate the 50-year wave; taking the ratio D_9/D_{21} removes the 50-year variation and leaves the 20-year wave as in Fig. 3(b). This wave has maxima in about 1895, 1914, 1934 and 1954, very close to a 20.0-year period. The maximum in 1970 is a partially remaining one of a shorter period component. The minima of the 20-year wave are at more irregular intervals, in 1909, 1922 and

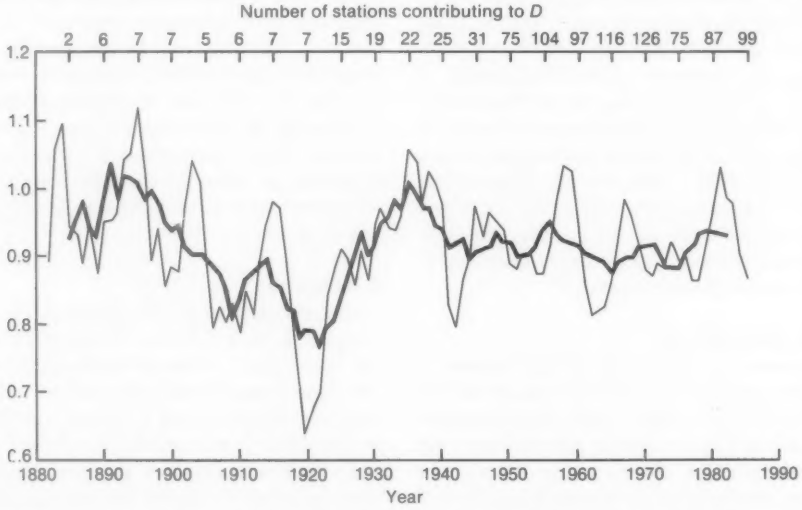

Figure 2. Running means of D over (a) 3 years (D_3) showing the combined contribution of the 7-, 11-, 20- and 50-year components (thin line), and (b) 9 years (D_9) showing the contribution of the 20- and 50-year components only (bold line). The number of stations from which the D values for each year are calculated are shown along the top of the figure.

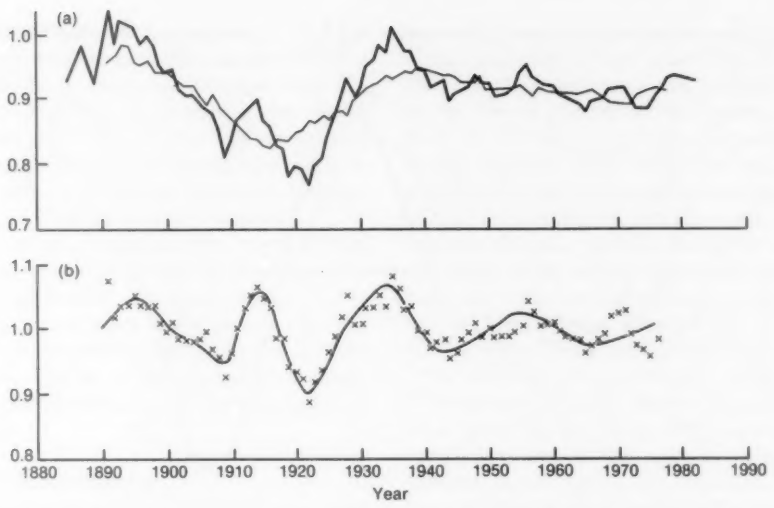

Figure 3. (a) Running means of D over 9 years (D_9) showing the contribution of the 20- and 50-year components only (bold line), and 21 years (D_{21}) showing the contribution of the 50-year component only (thin line), and (b) D_9/D_{21} reproducing the waveform of the 20-year wave alone.

1943. The mean amplitude over the whole interval is about 5%, after correction for a smoothing factor $f = 0.70$, increasing up to about 1920 and decreasing afterwards.

3.3 11-year period wave

It is not possible to isolate the 11-year wave using this process so an alternative method is used. D_3, in Fig. 2, contains all the four components at nearly full amplitude while in D_9, also shown in Fig. 2, the amplitude of the 7- and 11-year waves are considerably reduced by the factors given in section 3.2. The ratio D_3/D_9, plotted in Fig. 4 with a smooth curve estimated by eye, shows clearly the combined 7- and 11-year waves almost completely free of the influence of the 20- and 50-year waves.

In this combined waveform the maxima are separated by alternate longer and shorter intervals of approximately 13 and 9 years and the successive minima are narrower and deeper, and broader and shallower. The pattern of their combination repeats with little change over 104 years which suggests that the individual periods must be close to a fixed simple ratio, in this case 2:3, in order to preserve the phase relationship. These features can be reproduced, as shown in Fig. 5, by the expression $1.0 \times (\sin(360° \times n/10.8)) + 0.6 \times (\sin(360° \times n/7.2) + 45°)$, where n is in years, representing the addition of sine waves with periods of 7.2 and 10.8 years, which are

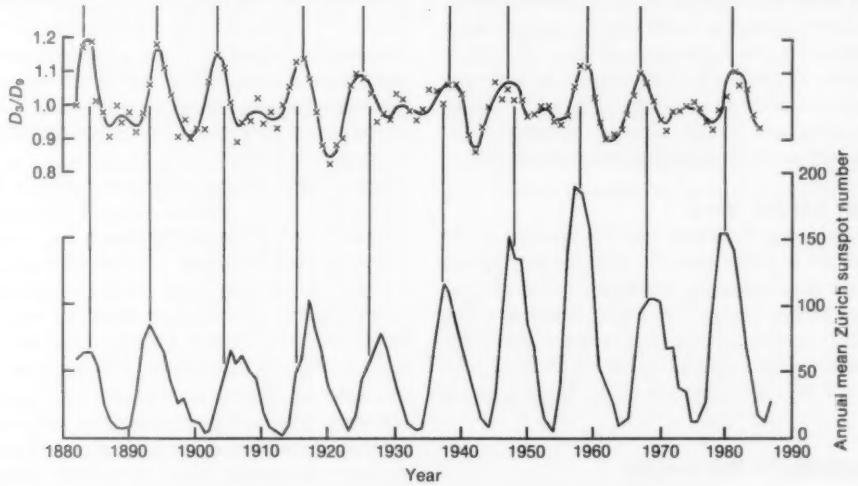

Figure 4. Upper trace, D_3/D_9 (D_3, D_9 as in Fig. 2), showing the combined waveform of the 7- and 11-year waves. Lower trace, the annual mean Zürich sunspot number. The upper vertical lines mark the years of maxima of the combined waveform; the lower vertical lines the estimated years of the maxima of the 11-year wave only.

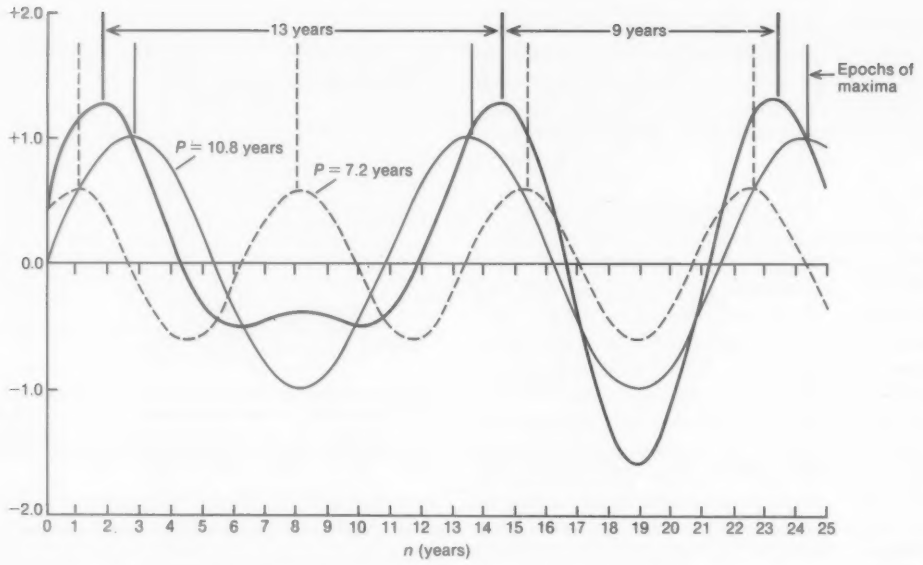

Figure 5. Synthesis of a combined 7- and 11-year waveform (bold line) from the addition of a 7-year sine wave (dashed line) and an 11-year sine wave (thin line) from the expression $1.0 \times \sin(360° \times n/10.8) + 0.6 \times \sin((360° \times n/7.2) + 45°)$, with n in years. The vertical lines show the approximate epochs of the maxima in the three waveforms.

in the exact 2:3 ratio. These two periods are within the ranges quoted in section 3. The factor 0.6 arises because the amplitudes of the waves are in the ratio 0.75, from Fig. 1, further modified by smoothing over 3 years (f for 7.2 years = 0.74, f for 10.8 years = 0.88, and $0.75 \times 0.74/0.88 \approx 0.6$). Fig. 5 shows that although the 7-year wave is relatively large the particular phase relationship of the two components is such that the combined wave still has only two prominent maxima in an interval of 21.6 years, i.e. 2×10.8 years, as observed.

The maxima of the 11-year wave occur one year before and after the maxima of the combined wave, from Fig. 5, and, from Fig. 4, they occur in years given approximately by the expression $1883 + (N \times 10.8)$ where N is the number of periods elapsed. In the same way the minima occur in the years $1888 + (N \times 10.8)$. The mean amplitude of this wave is estimated to be about 10% with possibly a small decrease since 1920.

3.4 7-year period wave

The curves in Fig. 5 indicate that the maxima of the 7-year wave are midway between, and one year before and after, the maxima of the combined 7- and 11-year waves. From this property, from Fig. 4, the years of the maxima and minima of the 7-year wave are given approximately by the expressions $1881 + (N \times 7.2)$ and $1884 + (N \times 7.2)$. The amplitude of this wave is about 7%.

4. Applicability of the results

To check the reality of these variations D values were calculated from one half of the original number of stations by taking the alternate ones from their arrangement in order of station number. Although this shortens the total record length, the frequency spectrum still shows components with periods very close to those reported above but with slightly different amplitudes.

These periodic variations of D can be detected even before 1920 when there were only 9 stations contributing observations (no more than 7 in any year). These stations are widely distributed over the United Kingdom, at Falmouth (Cornwall), Kew Observatory and Camden Square (London), Skipton (West Yorkshire), Eskdalemuir (southern Scotland), Aberdeen (eastern Scotland), Ben Nevis and Fort William (western Scotland) and Armagh (Northern Ireland). The widespread distribution of these stations suggests that the variations are synchronous over most of the United Kingdom. The number of stations increased rapidly after about 1930 and so it is expected that the D values are consequently less liable to error after that time.

During the data extraction it was noticed that, except for stations in the extreme west of England and Wales, and north-west Scotland, the annual maximum amounts occurred most frequently ($> 80\%$ of occasions) during the summer months from April to September within events whose short durations from 1 to 3 hours suggests that they were intense convective rainfalls. There were too few stations to establish whether these variations also occur in extreme amounts from frontal rainfall.

It seems implausible that the variations described here are experienced by only the annual maxima and not, for instance, the second, third, etc. largest rainfalls in each year which may not be much smaller than the maxima, and so it is likely that they are present in all large 1-hour duration rainfalls.

5. Related observations

Median normalized 2-hour rainfall amounts from 22 unspecified stations in south-east England from the Flood Studies Report have been used to give the D_3 values from 1952 to 1969 in Fig. 6. They are in good agreement in amplitude with the values, also in Fig. 6, for 1-hour rainfalls, the corresponding maxima and minima differing in epoch by one year or less.

Lightning is often associated with extreme short duration convective rainfalls, and its occurrence in Britain has been studied by Stringfellow (1974). Running means over 5 years of his annual lightning incidence index, the number of flashes per unit area per year, are also shown in Fig. 6. They are highly correlated with D_3 for 1-hour rainfalls over the whole period from 1933 to 1971.

6. Origin of the variations

The dominant component of period 10.8 years, with maxima repeating strongly throughout the 104-year record as in Fig. 4, suggests a connection with solar activity. One measure of this activity is the Zürich sunspot number which has a dominant frequency component with $P = 11.1$ years (Herman and Goldberg 1978).

The annual mean Zürich sunspot number, Z, is plotted in Fig. 4. There is a clear correspondence even between the combined 7- and 11-year waves (D_3/D_9) and Z, extending over ten maxima. The lower vertical lines in Fig. 4 are estimated epochs of the maxima of the 11-year wave alone; for six out of the ten maxima the epochs for Z and this wave agree within one year, bearing in mind the limitation in time resolution imposed by using annual maxima for rainfalls and annual means for sunspot numbers. For the remainder the maximum difference is two years, occurring at times when the background variation is changing most rapidly.

The size of the maxima in D_3/D_9 do not show the gradual increase from 1880 to 1960 of the maxima of Z in its original units. If the 3-year running mean of Z is expressed relative to the 9-year running mean, analogous to D_3/D_9, then this does have the same appearance as D_3/D_9 with a nearly constant amplitude. The running mean of Z over 9 years represents well the background variation implied in Fig. 4 which has a period of about 180 years (Herman and Goldberg 1978) but a variation of this period cannot be resolved in the frequency spectrum of D because it is too long compared with the record length. It must be stressed that Z is only an indicator of activity displayed by many solar phenomena such as the emission of charged particles and electromagnetic radiation, and the strength of magnetic fields.

Currie (1988) reports variations with period 10.6 years and variable amplitude in monthly rainfalls over the last 100 years for many stations in the north-east United States. There are prominent maxima in the years 1881, 1892, 1905, 1916, 1927, 1937, 1948, 1958, 1968 and 1979 agreeing well with those estimated for the 11-year wave from Fig. 4. Currie (1987) also finds a strong variation of period 10.8 years in the level of the Nile summer flood during the interval 1690 to 1962, presumably related to rainfall in the African highlands. He attributes both of these variations, which have periods within the ranges quoted in section 3 to the 11-year period of solar activity; Stringfellow (1974) also suggests that the variation of lightning incidence index in Fig. 6 has the same origin.

The spectrum in Fig. 1 also shows small amplitude variations with periods from 5.0 to 6.0 years, i.e. about one half of the solar activity cycle period. The spectrum of Z also has a small component with period 5.5 years and some meteorological phenomena show variations with this period (Herman and Goldberg 1978).

Atmospheric luni-solar tides governed by the 18.6-year period of revolution of the moon's orbit with respect to the ecliptic have been suggested by Currie (1988) as the origin of a variation of period of 19.2 years and amplitude 5% in the north-east United States monthly rainfall records and a period of 19.8 years in the level of the Nile summer flood (Currie 1987). These both show maxima near 1916, 1936 and 1955 in good agreement with the maxima of the 20-year wave in Fig. 3. Again these observed periods are well within the ranges given in section 3.

A search of the literature has failed to reveal any description of a 7-year period variation in atmospheric phenomena. Its apparent close relationship of period to

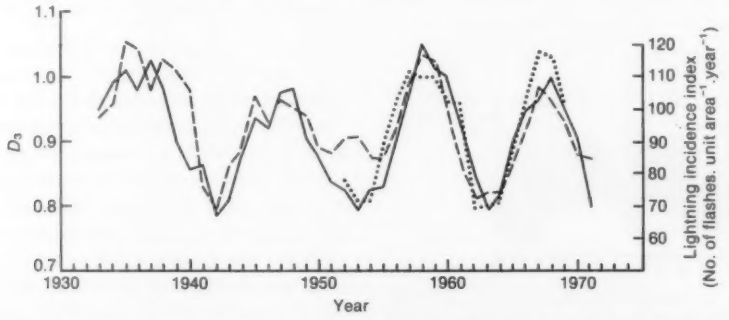

Figure 6. Comparison of D_3 for 1-hour (dashed line) and 2-hour (dotted line) rainfalls and the lightning incidence index (continuous line).

the 11-year variation suggests that the two waves have some common factor. For instance it has a period about one third of the double solar activity cycle of close to 22 years, which has been observed in such phenomena as the magnetic polarity of bipolar sunspot groups, geomagnetic activity and the intensity of cosmic rays (Herman and Goldberg 1978).

The 50-year period of the remaining variation suggests a climatic effect, of unknown cause, and again no evidence of observations of other phenomena with the same period have been found.

7. Conclusions

Annual maximum 1-hour duration rainfalls observed during the interval 1881 to 1986 over the whole of the United Kingdom appear to have four main components, approximately sine wave in shape, with periods of about 7, 11, 20 and 50 years and mean amplitudes of 7%, 10%, 5% and 7%. The two longer period components have decreased considerably in size since about 1935 and are now nearly undetectable, but the two shorter period components have decreased in size only slightly. These variations are believed to affect most large convective rainfalls and to be synchronous over the United Kingdom.

The maxima of the 11-year period wave have repeated strongly throughout the interval covered by the observations, and are closely synchronized with the maxima of the solar activity cycle.

The next prominent maximum of extreme rainfalls should occur in 1990, one year ahead of the next sunspot maximum which is expected to be in 1991, from Fig. 4. The prediction of the epoch of maximum sunspot activity is always uncertain though and it should be noted that judging from the large initial rate of increase since 1986, the next maximum of Z could occur as early as late 1989 (Gribbin 1988).

Apart from the intrinsic interest of these results they have practical relevance. Large one-hour rainfalls are important in causing flood events in some urban catchments with a response time of about this duration. For instance, for 1-hour duration rainfalls in locations in southern England there is an average interval (the 'return period') of 20 years between exceedances of 27 mm. If this is the threshold amount required to produce a flood in a particular catchment then for rainfall amounts increased by 10% (comparable to the magnitudes of the variations described here) the return period decreases to 17 years, and increases to 31 years for a 10% decrease in rainfall amount. These changes in return period can have important consequences for the design of flood control structures and the risk of their failure.

References

Currie, R.G., 1987: On bistable phasing of 18.6-year induced drought and flood in the Nile records since AD 650. *J Climatol*, **7**, 373–389.

—, 1988: Periodic 18.6-year and cyclic 10 to 11 year signals in Northeastern United States precipitation data. *J Climatol*, **8**, 255–281.

Gribbin, J., 1988: Return of sunspots bring radiation fears, *New Scientist*, **119**, No. 1620, p.22.

Herman, J.R. and Goldberg, R.A., 1978: Sun, weather and climate. Washington DC, NASA, Publication No. SP-426.

NERC, 1975: Flood studies report, Volume II, Meteorological studies. London, Natural Environment Research Council.

Stringfellow, M.F., 1974: Lightning incidence in Britain and the solar cycle, *Nature*, **249**, 332–333.

551.543.5:551.553.5:551.515.82(411.1)

An investigation into an unusual pressure fall over Shetland

A.J. Gair
Meteorological Office, Lerwick

Summary

On 8 January 1988 a short-lived sudden fall of atmospheric pressure was observed over the whole of Shetland. Descriptions of the event and of an investigation to establish its cause are given.

1. Introduction

Sudden large falls of surface pressure, not obviously associated with the passage of fronts or troughs, are relatively rare. One such event on 25 January 1977 over south-eastern England has been described by Harvey and Warren (1978) who concluded that the pressure changes were caused by an atmospheric gravity wave, rather like the ripple formed when a small stone is tossed into a pool. In that example the wave travelled east-north-eastwards for several hundred kilometres with a speed of 32 m s^{-1}.

A similar event occurred on Friday 8 January 1988, the first indication being a sudden fall of pressure and change of wind direction and speed observed at 0650 GMT at Lerwick Observatory. Barogram and wind records, where available, were then requested from all observing stations in Shetland and Table I records the data extracted. In most places the fall exceeded 4 mb within a few minutes.

Table I. Pressure and wind changes over Shetland

Station	Mean wind change (deg./kn)		Pressure change (mb)	Time (GMT)
	From	*To*		
Fair Isle	180/28	150/23	−4.2	0640
Sumburgh	170/28	140/25	−3.9	0650
Lerwick	190/26	170/23	−3.5	0650
Sella Ness	180/26	140/16	−4.3	0650
Collafirth Hill	No record available		−4.4	0650
Muckle Flugga	No record available		−4.2	0650

Immediately afterwards the pressure started to rise. At the same time the surface wind backed about 20 degrees but then returned to its original direction during the following hour. No other significant changes took place at the time.

The wind speed generally decreased at the time of wind shift but rose again immediately after to about its previous level. This effect was most marked at Sella Ness. All barogram traces were remarkably similar, showing a small rise followed by an almost instantaneous fall, followed by a significant rise. The barogram and anemogram from Sella Ness are shown in Fig. 1 and Fig. 2, respectively, to illustrate the event. The apparently smaller fall of pressure at Lerwick

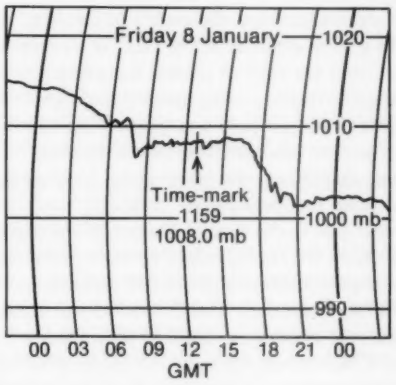

Figure 1. Diagrammatic representation of a portion of the barograph trace from Sella Ness meteorological office (60° 27′N 01° 16′W) for the period of interest. Note that the trace is running about 1 hour ahead of time.

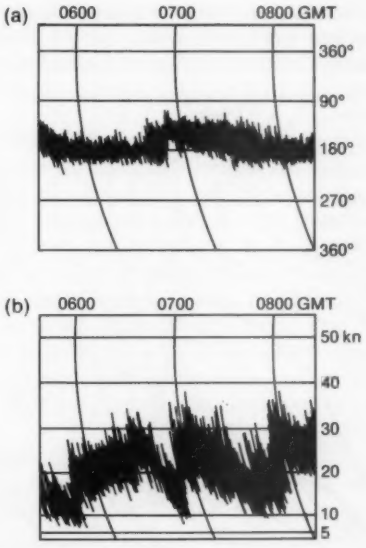

Figure 2. Diagrammatic representation of (a) wind direction, and (b) wind speed traces from Sella Ness for the period of interest on 8 January 1988.

may have been due to the use of a marine barograph with greater damping.

Mr Wheeler, the auxiliary observer on Fair Isle, noticed the event as it was happening and was able to read pressures (both converted to mean sea level) at 0650 GMT (1009.6 mb) and 0658 GMT (1007.2 mb), a drop of 2.4 mb in 8 minutes.

2. Synoptic situation

At 0001 GMT on the morning of 8 January, a strong, broad south-westerly jet was propagating north-eastwards across the Atlantic towards the north of Scotland. At the same time, the surface analysis showed a deep depression to the south of Iceland, an old, occluded front moving north-east across Iceland and Faeroe, and a second occlusion from the centre of the low, running south to a triple point at 56° N, 12.5° W. A ridge of high pressure over the eastern United Kingdom was rapidly declining and moving away quickly into the North Sea.

By 0600 GMT (Fig. 3) a strengthening south-south-westerly airflow was becoming established over Shetland with the centre of the depression over south-west Iceland and the associated, occluded front running south-east, just to the west of Faeroe, to the triple point at 57.5° N, 6° W. The midnight Lerwick ascent showed strong, warm advection from the surface to 500 mb (Fig. 4). At this time the low-level air mass over Shetland was unstable compared with the sea temperature of 9 °C, but topped by an inversion at 800 mb and a second just below 750 mb. Further to the west, the midnight Stornoway ascent (not shown) showed an inversion at 950 mb with the air mass conditionally unstable from about 900 mb to 600 mb. However, the ascent steadily 'dried out' from 950 mb up to 600 mb.

The occlusion appeared to pass through Lerwick from the west just before midday with a small rise in temperature and dew-point but no noticeable change in wind speed and direction. It is therefore reasonable to assume that the Lerwick midday ascent, launched at 1115 GMT, was representative of the air mass just ahead of the occlusion at low level.

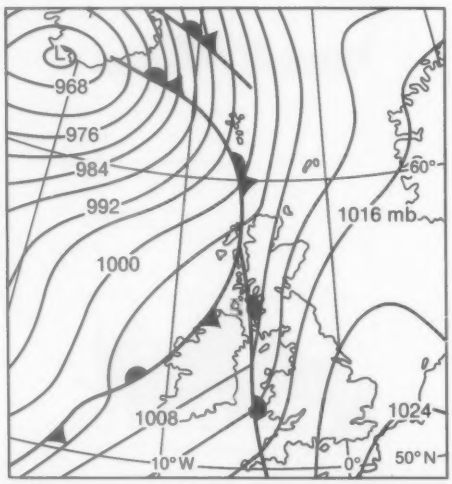

Figure 3. Surface synoptic situation for 0600 GMT on 8 January 1988.

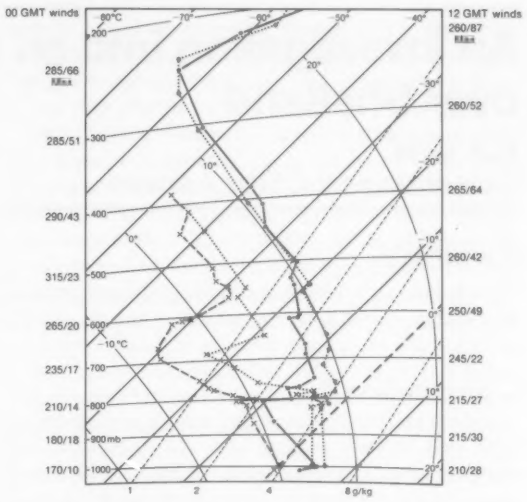

Figure 4. Radiosonde ascents made at Lerwick on 8 January 1988; the solid and dashed lines show the 0000 GMT ascent, and the dotted lines show the 1200 GMT ascent. The direction (deg.) and speed (kn) of the wind are shown.

3. Further observations and discussion

It was decided to examine barograms from stations to the west of Shetland, as far south as 57° N, and also from Faeroe, Norway and the North Sea oil installations. The results are summarized in Table II.

Table II. Pressure changes at stations other than in Shetland

Station	Pressure change (mb)	Time (GMT)
St. Kilda	−1.0	0100
Benbecula	−1.5	0310
Stornoway	−1.8	0340
Butt of Lewis	−2.2	0345
Neist Point	−4.0	0400
Diabaig	−1.5	0430
Cape Wrath	−3.5	0445
Wick	−3.0	0555
Kirkwall	−3.0	0600
Dalcross	−3.8	0600
Aviemore	−0.7	0630
Vagar (Faeroes)	−1.5	0630
Lossiemouth	−1.2	0655
Kinnaird Head	−1.0	0810
Thistle Alpha	−3.5	0900 *
Pacesetter 4	−4.0	0900 *
Hellisøy (Norwegian lighthouse)	−1.3	1200
Bergen	−1.0	1220
Utsira (Norwegian lighthouse)	−0.7	1340

* Approximate time as no time-marks etc. on barogram.

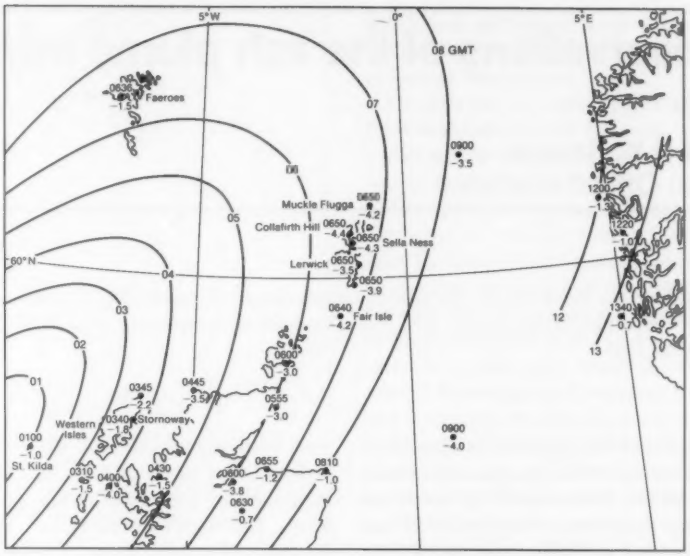

Figure 5. Isochrones of the arrival of the pressure fall, with spot positions of time (GMT) and fall (mb). Some of the places mentioned in the text are marked.

These data, together with the Shetland reports, were plotted and isochrones drawn as shown in Fig. 5.

One of the striking things about this event is the extraordinary similarity of most of the barogram traces examined, and also the strong resemblance to the trace from the event over south-east England in 1977.

Two possibilities for the origin of this event have been considered. Firstly, that it might have been induced by the strengthening south-south-westerly airflow over the Scottish mountains, but this was soon discounted by its appearance at St. Kilda and the Western Isles. However, it is suspected that the mountains may have played a part in increasing or decreasing the amplitude and rate of movement as the wave moved eastwards.

The second possibility was that the gravity wave was initiated by the frontal system advancing from the west, i.e. at the boundary between air masses of different density. This would agree reasonably well with the St. Kilda report at 0100 GMT — although some way ahead of the surface position of the front.

The pressure falls at Stornoway and the Butt of Lewis, appeared to coincide with the frontal passage as there was a veer of wind of 20 degrees and a significant rise in dew-point. At Kirkwall and Wick there were no changes to indicate the passage of a surface front; and in the case of Shetland, the front did not pass through until between 1100 and 1200 GMT, long after the gravity wave.

From examination of the surface pressure charts of the Central Forecasting Office, Bracknell, the triple point moved east-north-east at an average speed of about 20 m s^{-1} between 0000 and 1200 GMT. An examination of the isochrones in Fig. 5 shows that the average speed of movement of the onset of the sudden pressure fall was about 26 m s^{-1} to the north-east, along a line from St. Kilda to Muckle Flugga. This figure for the rate of movement must be considered unreliable due to the lack of information to the north-west of Scotland. Also, its rate of travel would appear to have been erratic and less than the frontal speed at times — leading to the front catching up at Stornoway and the Butt of Lewis.

It would therefore seem possible that the gravity wave was initiated at, or near, the frontal surface as it intersected the sea: it then propagated and amplified ahead of the front in the stable air under the inversion at 800 mb, evident on the 1200 GMT Lerwick ascent.

4. Conclusion

It is suggested that a gravity wave was initiated at, or close to, the frontal surface, possibly at the triple point, and that it propagated north-east and amplified in the stable air below 800 mb, the rate of propagation being generally considerably greater than the frontal speed. Over the more mountainous areas of northern Scotland there is evidence to suggest that the gravity wave lost some of its identity due to topographical effects. It is also possible that some of the largest pressure falls went unrecorded over the sea to the north-west of Scotland.

Acknowledgements

I wish to thank the many individuals who have helped by supplying advice and much of the basic data.

References

Harvey, I.G. and Warren, D.E., 1978: Observations of rapid pressure variations: 25 January 1977. *Weather*, **33**, 11–17.

551.508.81:551.510.42(424):634.0.43

Radar observations of the ash plume from a large fire

P. Evans and P.K. James
Meteorological Office, Bracknell

Summary

A large Army warehouse at Donnington, Shropshire caught fire on 25 April 1988. The plume of ash from the fire was observed by the weather radar situated at Clee Hill. The radar measurements show the evolution of the plume and its subsequent dispersal.

1. Introduction

On 25 April 1988 a fierce fire broke out in a hangar at an Army store at Donnington in Shropshire (National Grid Reference SJ710130). Press reports indicated that the fire caused damage valued at or about £100 M and it resulted in asbestos and ash being distributed over an area of more than 100 km^2 of the surrounding countryside. The incident received national publicity which highlighted public concern over the spread of asbestos.

The fire produced a cloud of smoke and ash, which rose to an altitude of over 2000 m. Radar echoes from the ash cloud were picked up by the Clee Hill weather radar and appeared in the 5 km resolution national weather radar composite. Information from a number of higher elevation scans and some data with 2 km resolution are recorded on site for off-line analysis; these data were used to study the evolution of the cloud in greater detail.

2. Radar data collection

The Clee Hill weather radar operates at C-band (5.6 cm wavelength) and has a beam width of 1.0°. Every 5 minutes the radar performs a series of 4 PPI* scans in sequence at elevation angles of 2.5°, 1.5°, 0.9° and 0.0°. Fig. 1 shows a vertical section through the radar beams over Shropshire. Above Donnington, which is 37 km north-west of Clee Hill, the centres of the beams are at 2230 m, 1580 m, 1200 m and 615 m above sea level. The beam has a circular cross-section which at this range is 650 m wide between the one-way full-width half-power points.

Data are collected in polar co-ordinates with a resolution of 187 m in range by 1.0° in azimuth, and corrections are made to allow for range effects, ground clutter and attenuation. The relative strengths of the reflected and transmitted radar waves are a measure of the radar reflectivity factor which is converted to an equivalent rainfall rate. Finally the data are mapped from polar co-ordinates on to Cartesian grids of 2 km and 5 km resolution. Grid data with 5 km resolution from all four elevation scans are archived on magnetic tape together with 2 km resolution data from the 0.0° scan. Real-time estimates of surface rainfall are transmitted to local users at 5-minute intervals and to the central radar networking computer, RADARNET, every 15 minutes.

For the present analysis the recorded rainfall rates were converted back to radar reflectivity factors (Z). The analysed data are shown in dBZ where $dBZ = 10.0 \log_{10}(Z)$. During the Donnington fire the observed dBZ values ranged from the minimum detectable of 3 dBZ up to a maximum of 38 dBZ.

3. Synoptic situation

Fig. 2 shows the synoptic situation at 1200 GMT on 25 April 1988. High pressure over southern England was giving way as a weak trough approached from the north-west. At Shawbury (17 km west-north-west of Donnington) the 10-minute average 10-metre wind varied in direction between 050° and 115° during the period of the radar observations, the mean wind being 095°/3.0 m s^{-1}. The 1200 GMT Aughton radiosonde sounding showed a weak inversion at 903 m. Immediately above the

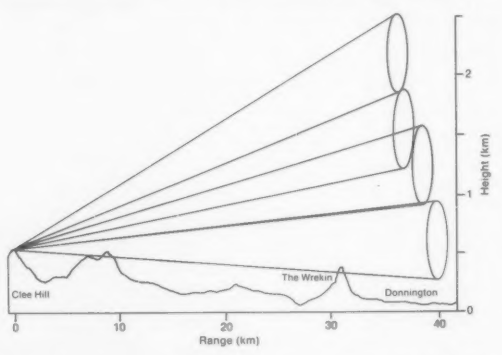

Figure 1. A vertical cross-section through the Clee Hill radar beams over Shropshire. The radar performs PPI scans at elevation angles of 2.5°, 1.5°, 0.9° and 0.2°. Above Donnington (70 m AMSL) the centres of the beams are at 2160 m, 1510 m, 1130 m and 545 m above ground level, and the beam is 650 m wide.

* PPI or Plan Position indicator is a circular picture produced by scanning a radar beam through 360° in azimuth at a low elevation angle.

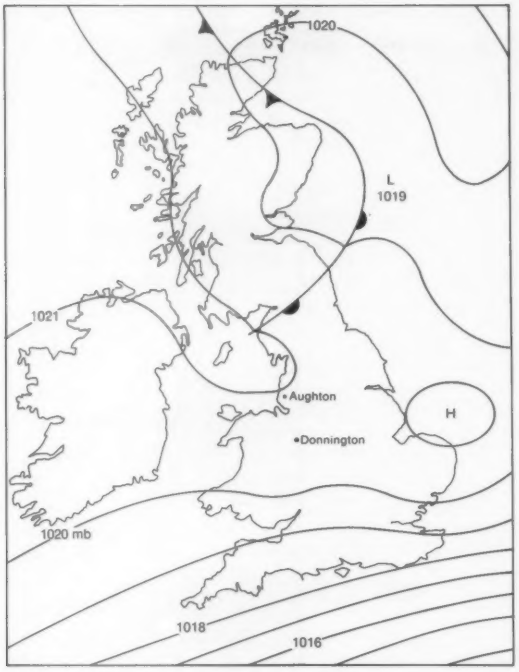

Figure 2. Synoptic situation at 1200 GMT on 25 April 1988. Isobars are at 1 mb intervals. The locations of Donnington and Aughton are shown.

inversion the wind was 095° / 5.7 m s^{-1} and at 2169 m it was 080° / 5.2 m s^{-1}. Above this height the wind backed steadily to 320° / 6.2 m s^{-1} at 4300 m. All the air in the lowest 3 km was sufficiently dry such that lifting to 3 km height would not cause saturation.

4. The radar observations

Fig. 3 shows the sequence of observations made over Shropshire by the 0.0° elevation scan at intervals of 5 minutes. This sequence clearly shows the development of the plume, its motion and subsequent dispersion. The radar measurements provide a definite indication of the plume's presence in a given square but the absence of a measurable signal can either mean that the plume was absent or that its concentration was too low to be detected.

The fire started at about 1440 GMT and the sequence shows the plume expanding and spreading steadily westwards. Press reports indicated that by 1520 GMT the fire was at its most intense and between 1525 and 1545 GMT the strongest radar returns where observed. At approximately 1630 GMT the fire was brought under control and the generation of the ash cloud effectively ceased. The plume then 'broke away' from Donnington and the last observations were made at 1725 GMT near Shrewsbury.

Radar returns from the ash cloud were first detected at 1448 GMT within the 1.5° scan, having risen to this height (1580 m AMSL) since the previous 0.0° scan which was performed some 2.5 minutes earlier. This implies that the cloud must have initially risen at a rate of greater than 6.4 m s^{-1}.

On only two occasions (1531 and 1535 GMT) were returns observed in the 2.5° scan (2230 m AMSL), so it would appear that the bulk of the material in the plume was contained below 2000 m.

The 1535 GMT scan shows ash 15 km downwind of Donnington in a direction of 260°; this means that it must have moved with a mean speed of 5.3 m s^{-1} over the 47 minutes since the first observations were made. The plume's velocity could also be estimated by tracking individual features as in Fig. 4 which shows the average intensity of the radar return as a function of distance west of Donnington, at 5-minute intervals. Using Figs 3 and 4, peaks in the intensity patterns near Shrewsbury at 1625 and 1655 GMT could be traced backwards to give mean velocities of 075° / 4.8 m s^{-1} and 080° / 5.6 m s^{-1} respectively. These values can be compared with the 1028 m and 2169 m winds at Aughton which were 095° / 5.7 m s^{-1} and 080° / 5.2 m s^{-1}.

Fig. 5 shows the average intensity of the radar return observed over the whole period. Of some interest is the spread of the plume transverse to the mean wind direction. Examination of the 1525 GMT scan in Fig. 3 shows that the plume has spread over a sector of at least 45°.

5. Discussion

Radar returns as large as 38 dBZ were observed during the Donnington fire. If raindrops were the target this would imply a rainfall rate of around 10 mm h^{-1}, but the air was too dry for precipitation to have been generated.

Sufficiently sensitive weather radars are able to obtain measurements from 'clear-air'. These returns may be attributable to birds, insects or man-made chaff* but generally they are from gradients of refractive index (caused by gradients of temperature and humidity in the atmosphere) occurring on a scale comparable with half the radar wavelength (James 1980). Such returns are commonly observed by sensitive 10 cm wavelength radars in the boundary layer and in particular allow the observation of forced convection associated with stubble burning. Viscous damping however means that such returns are generally too small to be detected by conventional 5 cm weather radars. During the Donnington fire temperature gradients much larger than those occurring in the free atmosphere would have been generated so that it is possible that returns from 'refractive index homogeneities' may have contributed to the radar signal close to Donnington.

Press (*Shropshire Star*) and television coverage reported asbestos and ash particles several centimetres across scattered over the nearby countryside and indeed

* Chaff is a cloud of narrow strips of metalized foil normally launched by rocket or dropped by aircraft.

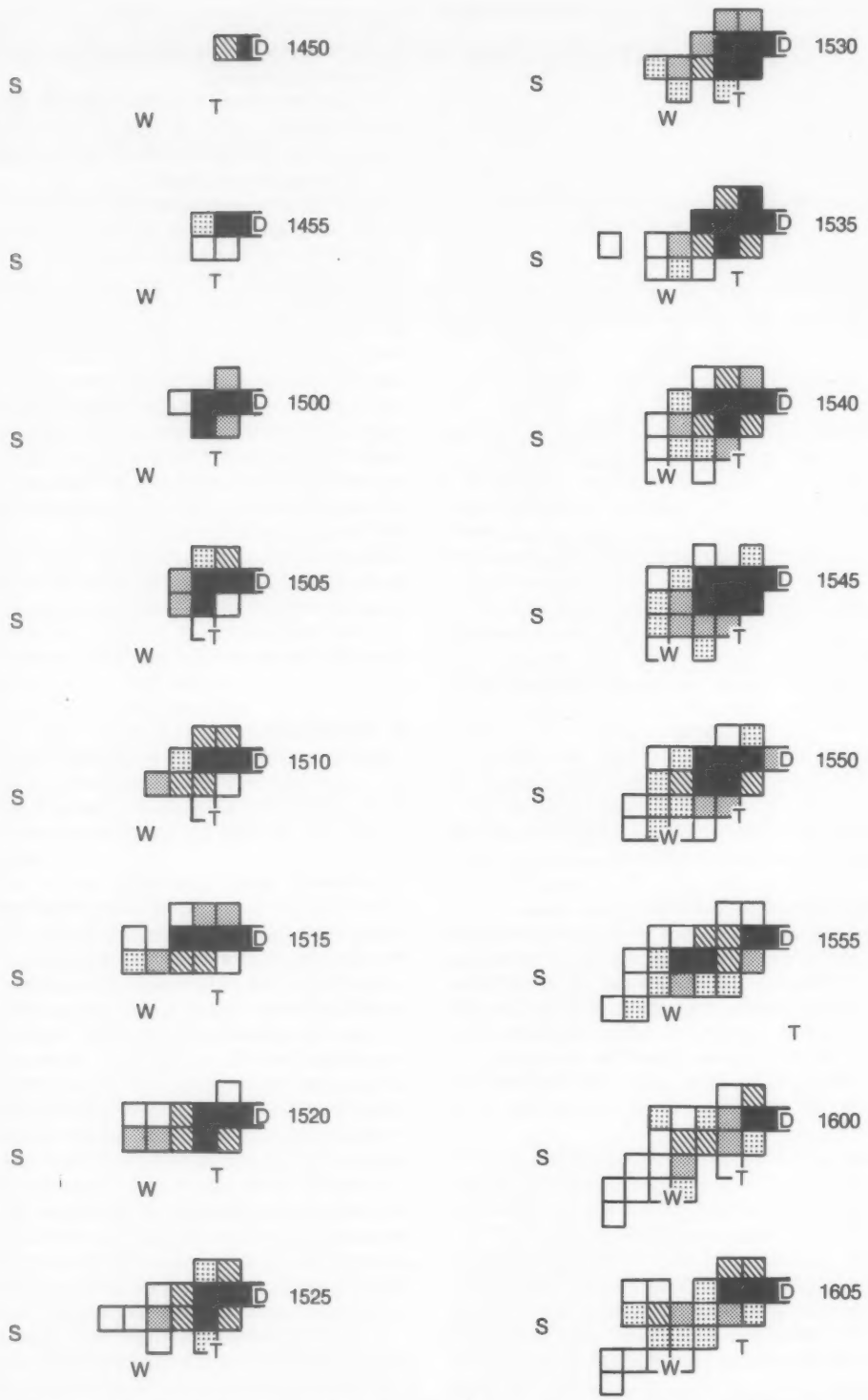

Figure 3. A sequence of radar observations made by the 0.0° scan at 5-minute intervals from 1450 to 1715 GMT. The locations of Donnington, Telford, The Wrekin and Shrewsbury are indicated by the letters D, T, W and S respectively. The radar observations on the 2 km mesh grid are shaded to indicate the strength of the return as shown in the key.

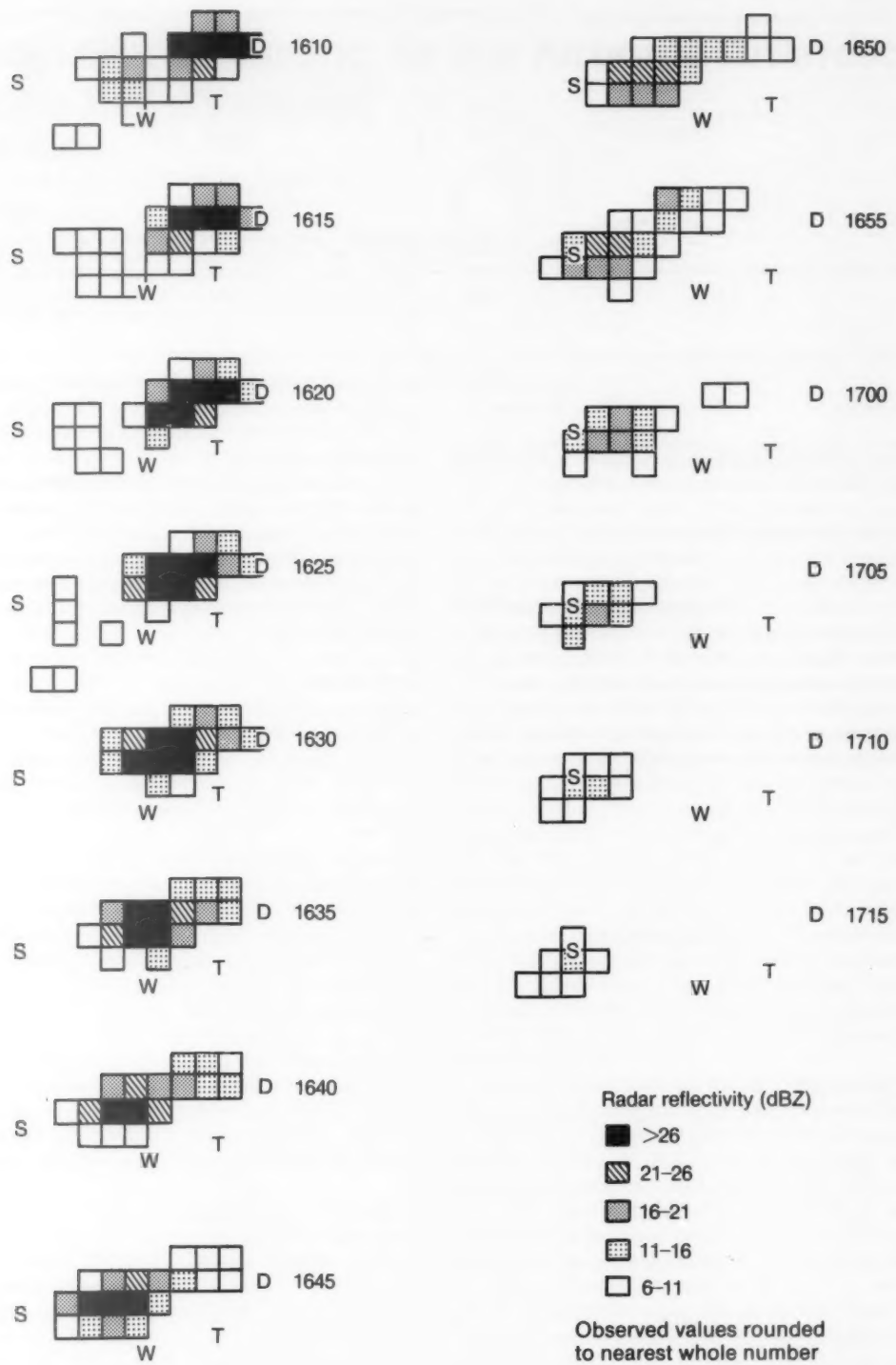

Figure 3 continued.

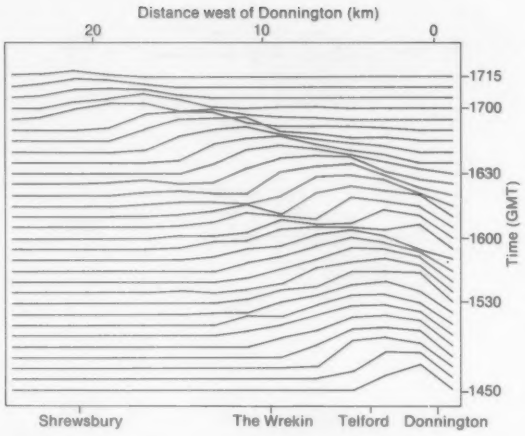

Figure 4. The intensity on an arbitrary scale of the radar return at 5-minute intervals averaged over all squares in the north-south direction as a function of distance west of Donnington.

such particles reached Shrewsbury which is more than 20 km from the source of the fire. The ash cloud over Shrewsbury was sufficiently dense that, for a period during the afternoon, the automatic street lights came on. Although asbestos and ash are relatively poor radar reflectors the large quantity of this material carried by the strong updraughts associated with the intense fire allowed it to produce an easily detectable return signal.

The fire occurred under relatively light wind conditions and the plume spread a considerable distance transverse

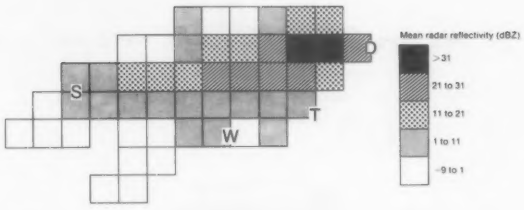

Figure 5. Average radar reflectivity observed over the period 1450 to 1715 GMT. For scale see key. This scale was chosen so that if the minimum detectable signal was registered in a 2 km square in a single 5-minute period then it would also appear on this figure. Each step on the scale corresponds to an increase in the mean radar reflectivity by a factor of 10.

to the mean wind direction. Such a spread highlights the problems which face forecasters attempting to predict the path of material following an event of this type in light wind conditions.

On this occasion the dispersal of a pollutant could be observed by the weather radar network. In general most pollutants — chemical, biological or nuclear — cannot be observed by weather radars. In principle, however, chaff could be introduced into the region where a release occurs then the subsequent dispersion could be directly tracked by radar.

Reference

James, P.K., 1980: A review of radar observations of the troposphere in clear air conditions. *Radio Sci*, **15**, 151–175.

551.509.58:551.507.352:551.510.534(99)

A note on forecasting for the Airborne Antarctic Ozone Experiment

P.R.S. Salter
Meteorological Office, Bracknell
S.D. Merrick
Meteorological Office, Royal Air Force Brize Norton

Summary

An account is given of forecasting for the Airborne Antarctic Ozone Experiment, and some simple comparisons are made between reported and forecast high-level winds over Antarctica.

1. Introduction

Ozone (triatomic oxygen) is a vital constituent of the earth's atmosphere. Although it is present in concentrations of only a few parts per million, ozone is able to absorb solar radiation at wavelengths shorter than about 310 nm. It therefore acts as a shield for the earth's biosphere and protects it from harmful ultraviolet radiation. Photochemical processes caused by solar radiation occur high in the atmosphere and reach a maximum at levels around 20 km, both to produce and destroy ozone. Ozone is initially formed when oxygen molecules dissociate into atoms, which then recombine with other oxygen molecules. Destruction of ozone occurs mainly as the result of catalytic reactions involving other gases. Some of these gases are unfortunately the breakdown products of man-made source gases.

International concern over the possible impact on the ozone layer by man-made source gases such as chlorofluorocarbons (CFCs) was first aroused in the late 1970s when research showed dramatic reductions in ozone concentrations during the Antarctic spring (Farman *et al.* 1985). This led to the signing in September 1987 of the Montreal Protocol. This agreement was signed by virtually all the CFC-producing nations, and commits them to a significant reduction in CFC output over the next few years.

Two basic but different theories have been advanced by atmospheric scientists to explain the observed reduction in the Antarctic ozone concentrations. These are:

(a) that large-scale circulation changes introduce air with low ozone concentrations such as might come, for example, from tropospheric sources, into the Antarctic stratosphere, or

(b) that the changes in the ozone concentrations are linked to changes in source gas concentrations, specifically compounds containing chlorine and nitrogen.

It was to investigate this so called 'ozone hole' that specially instrumented aircraft of the United States National Aeronautics and Space Administration (NASA) were tasked with making detailed measurements of elements considered vital to the explanation of why the sudden drop in ozone concentration at the end of the austral winter should occur.

2. Meteorological support

The Meteorological Office was involved in two important aspects. One was concerned with the theoretical science side of the experiment and involved the Atmospheric Chemistry Group at Bracknell. The other involved the flight forecasting problems and concerned the two forecasters who were deployed to Punta Arenas in southern Chile. A dedicated network of communication links between the USA, the United Kingdom and Chile was set up by Research and Data Systems Corporation under contract to the project management to provide the flow of data to and from the project staff at Punta Arenas. In particular, dedicated links were set up between the Regional Telecommunications Hub in Bracknell and Punta Arenas, and between the European Centre for Medium-range Weather Forecasts (ECMWF) and Punta Arenas. In the event of a breakdown on one of these links, Bracknell was also linked to ECMWF.

Host nation support was provided by the National Meteorological Service of Chile while the communication links to the United Kingdom allowed the numerical weather prediction (NWP) model products to be received from Bracknell, and also from ECMWF, in real time. The Meteorological Office coarse-mesh model products were provided twice daily for up to 72 hours ahead and fine-mesh model products once a day for up to 36 hours ahead. These products covered fields of surface pressure at mean sea level, and winds and temperatures at standard levels up to flight level (FL) 780 (78 000 ft). They were used operationally as the basis for flight documentation as well as for planning purposes. Like the products from the Meteorological Office, those from ECMWF were provided to cover standard levels up to FL780 but the forecasts were

extended up to 240 hours ahead. These ECMWF data were used primarily for determining 'weather windows' so that development of the plans for successive aircraft missions could proceed well ahead of the event.

The Atmospheric Chemistry Group provided routinely, charts of isopleths of isentropic potential vorticity (IPV) for different temperatures based on data from the Meteorological Office coarse-mesh model. These IPV data permitted a parcel of air sampled by a high-flying aircraft to be followed theoretically (i.e. assuming no mixing etc.) around the polar vortex, and to be considered for re-examination many days later by a further flight, weather permitting. Ozone measurements by satellite were also made available in real time at Punta Arenas through communication links to the USA, and added an important dimension to the scientific aspect of flight planning not experienced previously by the mission forecasters.

In addition the Chilean forecasting office in Punta Arenas provided routinely, plotted surface-weather charts and cloud pictures; the latter could be interpreted by colour-slicing techniques made available by the Chileans. The Chilean meteorologists also provided airfield forecasts and some upper-air data from Antarctica required by the project staff. Not least, a NASA radio station set up at Punta Arenas by the project management was in frequent contact with the US base at Palmer Station in Antarctica, which provided upper-air soundings in support of the project at a location close to a number of the aircraft flight paths.

3. Requirements for aircraft operations

NASA deployed two research aircraft to Punta Arenas during August and September 1987, a DC-8 and a modified version of the U-2 known as the ER-2. The ER-2 operated at altitudes up to 18.5 km and as far south as 72° S. The limit of 72° S placed on the ER-2 was primarily for safety reasons. The DC-8 operated at altitudes up to 11 km and made several flights to or near the South Pole.

The requirements of the two research aircraft for meteorological support were quite varied. Both required detailed forecasts of upper winds and temperatures at the planned operating levels which between them varied between FL240 and FL700. For take-off and landing the ER-2 required the surface wind speed to be no more than 25 kn with a cross-wind component no greater than 12 kn. Cloud-base criteria were not very restrictive, the only requirement being that the cloud base should be 200 feet or more above ground level, with visibility not less than 1500 m. In flight, forecasts of areas where clear air turbulence (CAT) might be encountered were required and, in addition, up-to-date forecasts for the planned diversion airfield of Puerto Montt. This airfield is located some 800 miles to the north of Punta Arenas. Finally, ambient temperatures below −85 °C were of significance since it was believed that these could cause crystallization of various lubricants used in the aircraft control mechanisms.

The requirements of the DC-8 were more flexible when it came to take-off and landing. Surface winds were preferred to be less than 34 kn with a cross-wind component no greater than about 23 kn. Cloud base should be over 500 ft above ground level and visibility more than 800 m. In flight, forecasts were required for the diversion airfield of Rio Gallegos in southern Argentina, in case of encounters with areas of CAT, and for ambient temperatures below −76 °C. Temperatures lower than this could have caused waxing of the aircraft fuel. Forecasts of areas free from dense cirrus cloud were also required. The forecasters had not expected extensive areas of cirrus cloud at high altitudes in the Antarctic stratosphere near the Pole but they were features of some of the flights, even on occasions extending up to the ER-2 flight levels and sometimes thick enough to obscure the sun. This led to a requirement for the forecasters to predict areas where dense cirrus was likely. Flight plans were then made to avoid such areas of cirrus since many of the onboard spectroscopic instruments required either a clear view of the sun or clear-column conditions above the aircraft in order to obtain good quality data.

4. Results

An example of a forecast surface pressure chart issued for a DC-8 flight on 2 September 1987 is shown in Fig. 1 with the associated coarse-mesh forecast of FL340 winds and temperatures in Fig. 2. The actual track of the aircraft is shown in Fig. 3 and the winds and temperatures encountered in flight in Fig. 4. Whenever possible the actual winds and temperatures encountered during flight were relayed back to the NASA radio station set up at Punta Arenas, from where they were relayed rapidly to Bracknell and ECMWF for inclusion in the next computer run, while the Chilean meteorologists forwarded the data to the Global Telecommunication System, for world-wide use. Owing to the vagaries of Antarctic radio reception, one such report was inaudible in Punta Arenas but was received by a station in Boulder, Colorado. This report was subsequently relayed back to Punta Arenas and in this roundabout way eventually to Bracknell.

The example in Fig. 4 provides a good illustration of the complexity of the upper-wind fields which were sometimes experienced over Antarctica. The model provided rather dubious guidance on this occasion. The west or west-north-westerly winds of around 50 kn between Tierra del Fuego and the Palmer Peninsula were well forecast, as was the position of a trough near the peninsula and a corresponding ridge over the Weddell Sea.

The model wind speeds were much too low on the south side of the trough though, and also too smoothed out. The aircraft encountered wind speeds of 60–80 kn from the north-east in an area where the model

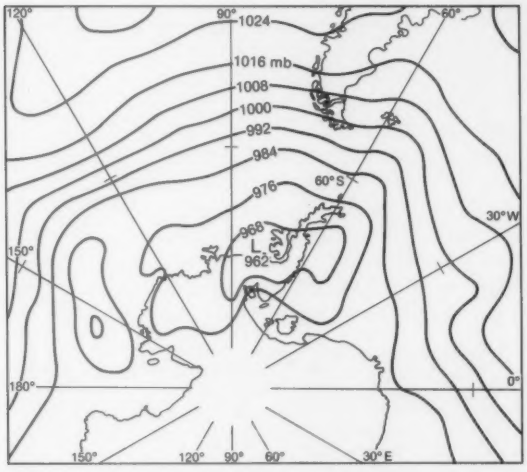

Figure 1. Forecast surface chart valid for 1800 GMT on 2 September 1987 issued for a flight by the DC-8 aircraft.

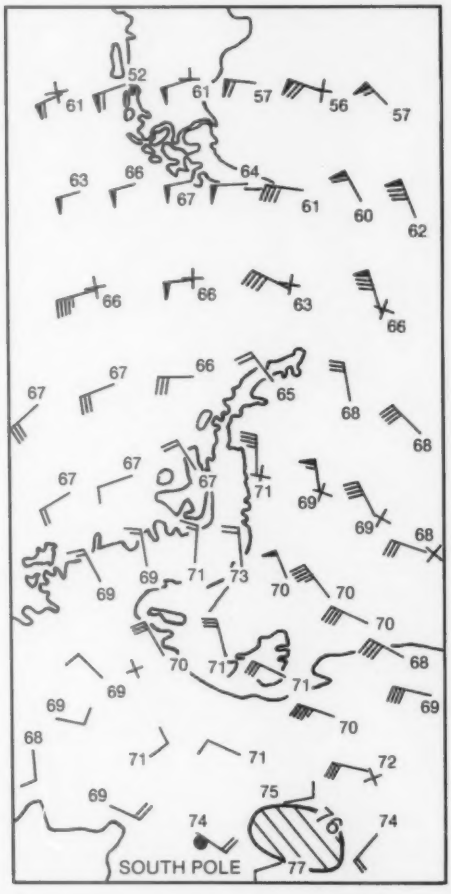

Figure 2. Coarse-mesh forecast chart for FL340 valid for 1800 GMT on 2 September 1987 issued in conjunction with the surface chart shown in Fig. 1. All temperatures shown (°C) are negative. The hatched area depicts an area of forecast temperature below −76 °C.

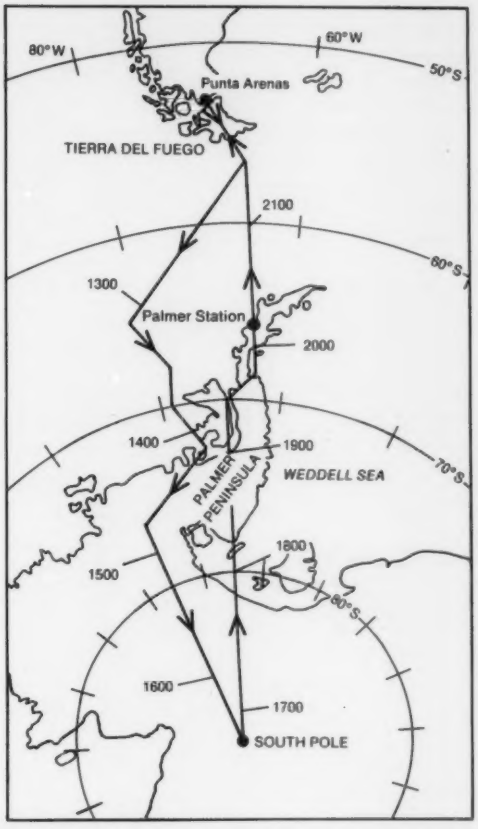

Figure 3. Flight track of the DC-8 aircraft on 2 September 1987 with times shown in GMT.

predicted a northerly wind of 15 kn. West-north-westerly winds of up to 83 kn quite close to the Pole were also a surprising feature of this flight and were not predicted by the model. The forecasters came to realize early in the project that an element of modification was required in forecast winds for the DC-8 which were frequently underestimated by the NWP products. On occasions this modification was to a significant extent and this was true particularly in relation to upper ridges, which were frequently predicted to have insufficient amplitude and wind strength over central Antarctica. The modification was based on interpreting all of the data to hand as well as partly a result of experience and of other flights, and was carried out by drawing modified isotachs on the documentation issued and providing charts of forecast jet-stream locations and strengths.

The forecasting of areas of high cirrus relied heavily on satellite information provided by the local Chilean forecasting office. This information was analysed and interpreted in conjunction with the Meteorological Office NWP products. It was found that the 150 mb forecast products were particularly useful in identifying likely regions of cirrus development penetrating the area

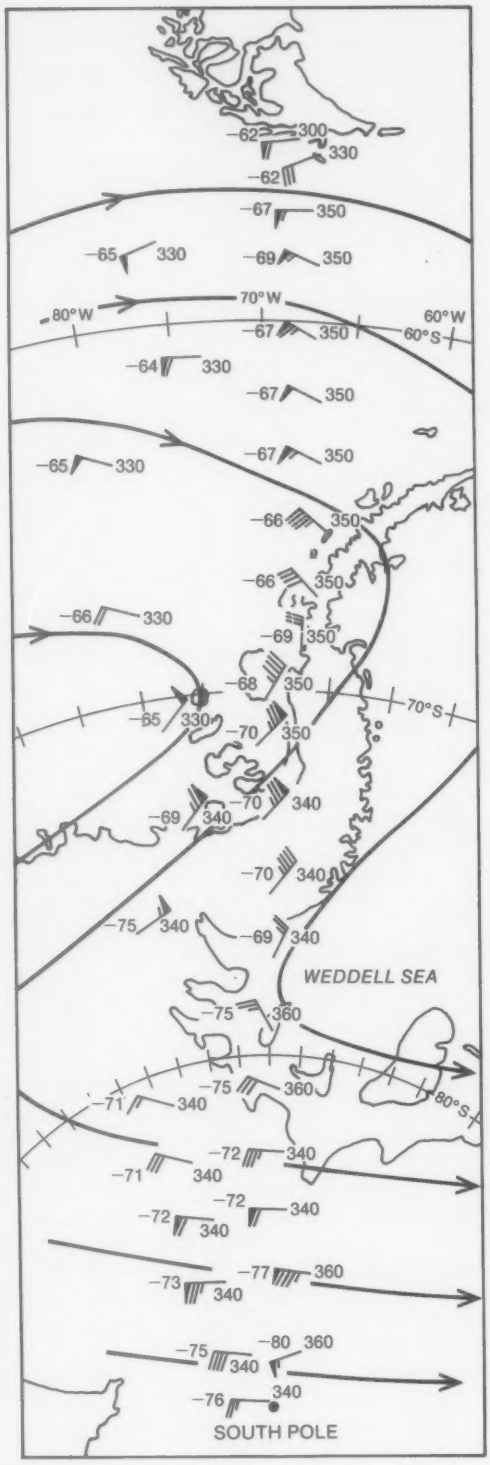

Figure 4. Actual winds and temperatures (°C) at stated flight levels, and inferred wind pattern (bold lines), encountered by the DC-8 aircraft during the flight on 2 September 1987.

over the Antarctic plateau. This was especially true when the forecasters successfully modified and extended the southerly range of high-amplitude upper ridges over Antarctica, since this permitted the DC-8 to be tasked to fly around the areas of thick cirrus and give the onboard spectroscopic instruments a clear view of the sun or clear-column conditions. Fig. 5 illustrates the track that the DC-8 was required to fly on a particular day so that it could operate in the right place and at the right time and avoid the cirrus.

Model performance at the higher levels flown by the ER-2 was surprisingly good, and examples are shown in

Figure 5. Cloud-temperature colour-slice showing the flight path of the DC-8 aircraft on 5 September 1987 which was successfully planned to fly to the east of the coldest cloud over the Palmer Peninsula and west of the cold cloud at the bottom right of the picture.

Table I. Winds and temperatures measured by the ER-2 aircraft compared with model forecast winds. Data from the aircraft are related to a validity time of 1800 GMT ± 3 hours.

	Forecast winds			Actual winds reported		
Position	FL	Wind (deg./kn)	Temp. (°C)	FL	Wind (deg./kn)	Temp. (°C)
17 August 1987						
56° S, 68° W	610	250/75	−70	610	245/76	−71
58° S, 66° W	610	250/80	−72	610	240/76	−74
60° S, 63° W	610	250/80	−75	590	245/68	−76
62° S, 63° W	610	250/80	−76	610	240/81	−76
64° S, 65° W	610	250/80	−79	610	245/100	−80
66° S, 68° W	610	260/75	−80	630	250/80	−84
28 August 1987						
57° S, 67° W	610	300/100	−63	560	300/82	−64
61° S, 70° W	610	310/95	−69	580	300/82	−70
64° S, 72° W	610	320/80	−74	600	304/75	−75
67° S, 75° W	610	330/75	−76	620	304/69	−77
70° S, 78° W	610	330/55	−78	630	307/63	−80
72° S, 80° W	610	330/55	−78	640	307/58	−81
9 September 1987						
55° S, 68° W	610	280/90	−73	610	272/86	−66
57° S, 67° W	610	290/90	−74	610	279/83	−69
60° S, 63° W	680	290/90	−76	660	283/94	−76
62° S, 64° W	680	280/75	−77	660	289/62	−74
63° S, 64° W	680	280/70	−78	660	284/60	−76
65° S, 64° W	680	280/55	−79	660	295/64	−80
67° S, 65° W	680	280/50	−79	660	280/50	−78
68° S, 65° W	680	310/35	−80	660	301/44	−79

Table I. Here the predicted values from the coarse-mesh model forecast issued to the pilot before take-off, are compared with the actual winds measured by aircraft sensors at various points along the flight track. Data for three flights are shown; those on the 17 August, 28 August and 9 September. These examples were chosen because on these flights the aircraft stayed near a flight level for which a forecast chart was available. Only the outbound leg is considered in each example since there was little variation on the return leg. Ignoring the difference in height between a standard flight level and that actually flown, it can be seen that there are a few occasions when spot differences between forecast winds and temperatures and aircraft reports are quite large. However, the most important point to emerge from a comparison is that the examples show that for each flight there is a mean vector difference of around only 10 kn and a mean temperature difference of around ±2 °C. This was most encouraging for the aircrew who came to expect a high standard as a routine.

5. Conclusions

At the outset of the project, it was expected that the notoriously windy weather at Punta Arenas and the environmentally severe problems of flying over Antarctica would severely restrict aircraft operations. In the event, twelve ER-2 flights were completed successfully which together with thirteen DC-8 flights provided a wealth of scientific data. Throughout the experiment the NWP products provided good guidance for the forecasters, especially at the high levels flown by the ER-2, and in part contributed significantly to the success of the experiment.

Acknowledgements

It is a pleasure to acknowledge the encouragement in particular of the aircraft pilots, the project scientist Dr A. Tuck of the Aeronomy Laboratory, NOAA, the project leader Dr R. Watson of NASA Headquarters, and Dr E. Condon the project manager, without which the forecasters would have found the task even more daunting. The ER-2 flight data were made available by K. Roland Chan of the NASA Ames Research Center, California. The Chilean forecasters and staff at Punta Arenas airfield provided a good deal of data which assisted the project forecasters' contribution to the experiment.

Reference

Farman J.C., Gardiner, B.G. and Shanklin, J.D., 1985: Large losses of total ozone in Antarctica reveal seasonal ClO_x/NO_x interaction. *Nature*, **315**, 207–210.

551.553.11(548)

Sea-breeze features over Sriharikota, India

T.R. Sivaramakrishnan and P.S. Prakash Rao
Meteorology Facility, Indian Space Research Organisation, Sriharikota, India

Summary

Using temperature, humidity and wind records since 1977 at the Sriharikota observatory, the occasions of occurrence of sea-breezes have been identified and their characteristics over the island have been studied. There are some differences in sea-breeze characteristics over Madras (70 km to the south) and Sriharikota Island. An attempt has been made to predict the sea-breeze occurrence over the island using the temperature and surface wind observations at 1000 hrs local time as parameters.

1. Introduction

Sea-breezes over the coasts are due to thermally driven mesoscale atmospheric circulation, for which differential heating is the essential requisite. A direct thermally driven circulation such as the sea-breeze occurs more frequently and with more regularity in the tropics than in middle and high latitudes. Since a moist air mass moves over the land during a sea-breeze, a change in temperature and humidity takes place and the wind direction is from the sea to the land. Thus, the sea-breeze moves as a front and can also be detected by radar under favourable radio propagation conditions.

The study of air motion in either mesoscale or any other scale of circulation forms an integral part of meteorology. Sea-breeze occurrence is an important event in environmental monitoring and aviation meteorology although it is a purely local phenomenon. Many climatological studies of sea-breezes have been attempted in India (Narayanan 1967, Dekate 1968, Ramakrishnan and Jambunathan 1958, Ramanadham and Subbaramayya 1965, Ramanathan 1931, Ramadoss 1931 and Roy 1941) and more general studies have been made elsewhere (Arakawa and Utsugi 1937, Brittain 1978, Hatcher and Sawyer 1947, Leopold 1949 and Marshall 1950)

Sriharikota (13.7°N, 80.2°E) is a rocket launching centre of the Indian Space Research Organization located as shown in Fig. 1. Many rocket launching operations and programme stages are dependent on the environmental conditions and hence for planning the operations efficiently a full investigation of sea-breeze fronts over the island was essential.

2. Data and methodology

Autographic weather records are available for the Sriharikota observatory since 1975. The temperature, humidity and anemograph charts of 1977–86 were scrutinized and the occasions of sea-breeze occurrence were identified by abrupt changes in these parameters. Some earlier sea-breeze reports (Venkataraman and Prakash Rao 1977, Prakash Rao 1985) were available for a few years but they were based on changes in relative humidity alone. First a statistical survey of sea-breezes was made. Later the characteristics of sea-breezes were derived in relation to the changes they bring about in meteorological parameters. The vertical extent of sea-breezes was also estimated from the pilot-balloon ascents which were made twice daily, one between 05 and 06 GMT and one between 09 and 11 GMT. The pilot-balloon wind data were available for the five years up to 1986. Occasions when sea-breezes set in after 06 GMT but well before the afternoon pilot-balloon ascent were considered and, from a comparison of the wind fields, an estimate of the vertical extent of sea-breeze fronts was attempted. Finally the probability of sea-breeze occurrence as a function of the morning wind and temperature data was investigated so as to develop forecasting methods for sea-breezes.

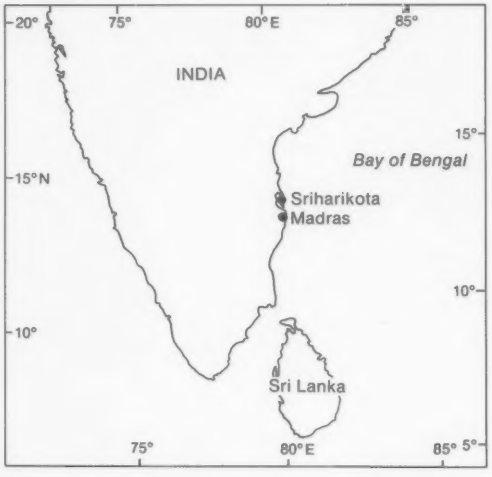

Figure 1. Location of Sriharikota and other locations mentioned in the text.

3. Results and discussion

3.1 Occurrence and detection

The number of occasions of a sea-breeze (1351 in total) were studied and their monthly frequency is

shown in Fig. 2. The first point to note is a maximum in the summer months of April and May. This is to be expected as the phenomenon is basically due to differential heating. Even during winter sea-breezes are detectable, although in limited numbers.

The occasions were sub-divided into the percentages in which they were detected by temperature and humidity change together, temperature change alone or humidity change alone, and these are shown in Table I. It can be seen that in the summer (April and May) and south-west monsoon (June to September) months, in only about 4 out of 5 occasions can the sea-breeze front be detected using both parameters. During November and the winter months, relative humidity alone is able to reveal the occurrence of the sea-breeze on most occasions. In February and December both humidity and temperature charts need to be monitored in order to detect the occurrence of a sea-breeze.

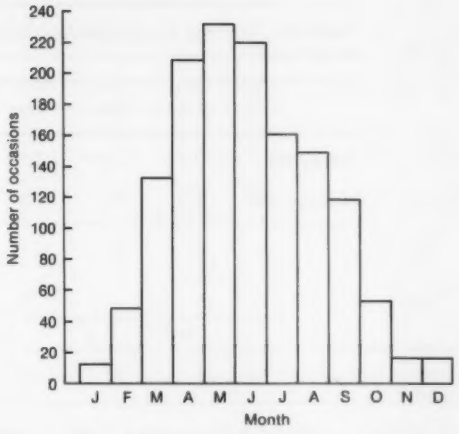

Figure 2. Monthly frequency of sea-breezes at Sriharikota, from the 1351 occasions studied in this paper.

3.2 Time of occurrence

Table II presents the distribution by time of sea-breeze arrival and Fig. 3 shows the average time of occurrence. Whilst the forenoon (1000–1200 hrs Indian Standard Time (IST)) is the more usual time of occurrence in April and May, as the south-west monsoon sets in and progresses in July and August, the time shifts to the mid-afternoon. For winter months the times begin in the late afternoon and advance again to near-noon in March. There is a temporary advance in time in September from 1515 to 1415 hours IST.

3.3 Fall of temperature

One of the advantages of the sea-breeze is the greater human comfort it brings about by lowering the temperature. There is a rapid fall in temperature taking less than 15 minutes between the fairly constant temperatures before and after the sea-breeze onset, and this can be determined accurately from thermograph records. The average and maximum falls found during the period February to October are shown in Table III. The maximum fall of temperature can be as high as 7.8 °C, but on average the fall is only about 3 °C in summer. The average fall in temperature shows a maximum in June. This differs from the tendency at Madras which has its maximum in mid-July (Rao 1955). The mean fall of temperature at Madras shows a wide seasonal variation from 1.1 °C in April to 4.6 °C in July. In comparison the range at Sriharikota is from 1.8 °C in February to 3.5 °C in June. The reason for the seasonal differences at Madras may perhaps be its urban nature, which is not the case at Sriharikota.

Table I. Percentage frequency of sea-breeze occurrence at Sriharikota, detected using different parameters

Detected by	Jan.	Feb.	Mar.	Apr.	May	June	July	Aug.	Sept.	Oct.	Nov.	Dec.
Humidity and temperature	0	27	59	72	81	83	83	77	79	36	12	—
Temperature alone	0	19	2	1	2	4	2	5	1	9	6	23
Humidity alone	100	54	39	26	18	13	15	18	20	55	82	77

Table II. Monthly distribution by time of the arrival of the sea-breeze at Sriharikota

Time (IST)	Jan.	Feb.	Mar.	Apr.	May	June	July	Aug.	Sept.	Oct.	Nov.	Dec.
1000–1159	0	10	55	123	111	23	8	2	18	8	0	1
1200–1359	4	31	64	78	84	62	36	40	40	16	1	3
1400–1559	2	6	10	4	20	59	58	36	27	15	8	3
1600 onwards	5	0	3	2	16	66	58	70	33	15	8	9

Table III. Average and maximum falls in temperature (°C) at the onset of the sea-breeze at Sriharikota

	Feb.	Mar.	Apr.	May	June	July	Aug.	Sept.	Oct.
Average fall	1.8	2.1	2.7	3.3	3.5	3.1	3.0	2.5	2.3
Maximum fall	3.8	5.0	7.2	7.8	7.7	6.5	6.0	6.5	3.8

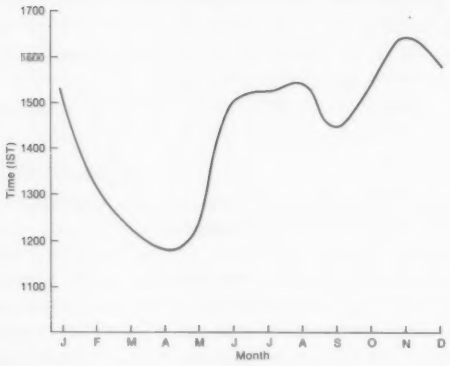

Figure 3. Average time (IST) of arrival of the sea-breeze at Sriharikota.

Table IV gives the average fall of temperature with the onset of a sea-breeze occurring in the specified time periods, i.e. forenoon, early afternoon, late afternoon, evening, and later. It can be seen that the fall in temperature at all times of occurrence over Sriharikota is a little less than that over Madras. However, the diurnal trend is exactly the same at both locations.

3.4 Winds

With the setting in of the sea-breeze the easterly component in the wind direction is dominant because of the influence of the large area of the Bay of Bengal to the east. While in about 66% of occasions a wind speed increase was noticed, a reduction occurred in the remaining occasions. If the westerly component was strong, the easterly sea-breeze component has to overcome the westerlies dynamically and perhaps this might be the reason for the reduction in wind speed, as the magnitude of the wind was considered irrespective of the direction. Of the total number of wind increases recorded with the sea-breeze front, on about 21% of occasions the speed increased by 3 m s^{-1} or more and on 55% of occasions the speed increased by 2 m s^{-1} or more.

Table IV. Average fall in temperature (°C) at the onset of the sea-breeze at Sriharikota and Madras, occurring within specific time periods

Time (IST)	Sriharikota	Madras*
1000–1159	2.2	2.6
1200–1359	2.9	3.0
1400–1559	3.3	3.7
1600–1759	3.5	4.7
1800 onwards	3.2	3.5

* From Rao (1955)

3.5 Vertical extent of the sea-breeze front

Upper-air wind profiles from pilot-balloon ascents could be constructed for most of the sea-breeze occasions during 1985 and 1986 and for a number of occasions in the early 1980s. The analysis showed that the depth of the atmosphere within which the sea-breeze could be detected (by changes in wind direction with height) over Sriharikota was never less than 100 m. The maximum observed depth of the sea-breeze front was 750 m (once in June and once in August). The greatest average depth of the sea-breeze occurs in May and is of the order of 400 m. It may be relevant that the highest insolation over Sriharikota occurs during May as suggested by the higher daily maximum temperatures.

Table V emphasizes the main salient points regarding the vertical extent of sea-breeze fronts during the summer and south-west monsoon months.

3.6 Forecast criterion

The temperature and surface wind at 1000 IST were noted and their correlation with the sea-breeze occurrence was investigated. Although the 0300 GMT (0830 IST) observation is the standard time for the morning synoptic observation in India, due to logistic constraints 1000 IST is the morning main observation hour for the Sriharikota launching range. The probabilities of the sea-breeze occurring within specified limits of ambient temperature are shown in Table VI. It is clear that if the temperature is greater than 31 °C at 1000 IST then, during the months of April to July, there is a good chance ($\geqq$72%) of a sea-breeze occurring on that particular day. Similarly from Table VII, which relates the probability of occurrence with surface wind speeds at 1000 IST, a wind speed of 6 m s^{-1} or more suggests a high probability ($\geqq$75%) of sea-breeze occurrence during the day, particularly during the months March to June. The two criteria put together will be helpful in forecasting the incidence of a sea-breeze on any particular day.

4. Conclusions

The average time of sea-breeze onset at Sriharikota is before noon for the summer months (April and May) which changes steadily to the afternoon in subsequent

Table V. Vertical extent of the sea-breeze at Sriharikota

	Apr.	May	June	July	Aug.	Sept.
Mean depth of sea-breeze (m)	270	400	330	320	340	290
Maximum depth of sea-breeze (m)	550	650	750	650	750	450
Percentage of occasions when sea-breeze front exceeds 400 m in depth	8	40	11	20	16	11

Table VI. Percentage probability of sea-breeze occurrence at Sriharikota in relation to the ambient temperature at 1000 IST

Temperature (°C)	Jan.	Feb.	Mar.	Apr.	May	June	July	Aug.	Sept.	Oct.	Nov.	Dec.
26–31	5	20	38	44	25	46	36	36	27	17	5	4
31–36	—	—	81	73	73	77	72	67	50	20	0	—
36–41	—	—	—	100	95	97	—	—	—	—	—	—

Table VII. Percentage probability of sea-breeze occurrence at Sriharikota in relation to the surface wind speed at 1000 IST

Wind speed ($m\ s^{-1}$)	Jan.	Feb.	Mar.	Apr.	May	June	July	Aug.	Sept.	Oct.	Nov.	Dec.
0–2	4	4	12	45	67	61	32	33	15	15	2	2
2–4	1	7	20	31	58	60	50	47	27	13	9	7
4–6	8	33	51	76	82	78	67	55	53	24	4	7
6–8	0	45	75	95	91	82	63	68	61	19	2	3
8 and above	0	0	0	100	83	75	67	50	50	0	7	6

months. The fall of temperature with the sea-breeze front can be as high as 7.8 °C with an average value of 3 °C. On only 4 out of 5 occasions do both temperature and humidity change with the arrival of the sea-breeze. A temperature of 31 °C or more with a wind speed of 6 $m\ s^{-1}$ or more at 1000 IST suggests a high probability of sea-breeze occurring on that day. Sea-breezes can be discernible up to a height of about 750 m over Sriharikota.

References

Arakawa, H. and Utsugi, M., 1937: Theoretical investigation on land and sea breezes. *Geophys Mag, Tokyo*, **11**, 97–104.

Brittain, O.W., 1978: Forecasting sea-breezes at Eskmeals. *Meteorol Mag*, **107**, 88–96.

Dekate, M.V., 1968: Climatology of sea and land breezes over Bombay. *Ind J Meteorol and Geophys*, **19**, 421–426.

Hatcher, R.W. and Sawyer, J.S., 1947: Sea breeze structure with particular reference to temperature and water vapour gradients and associated radio ducts. *Q J R Meteorol Soc*, **73**, 391–406.

Leopold, L.B., 1949: The interaction of trade wind and sea breeze, Hawaii. *J Meteorol*, **6**, 312–320.

Marshall, W.A.L., 1950: Sea breeze across London. *Meteorol Mag*, **79**, 165–168.

Narayanan, V., 1967: An observational study of the sea breeze at an equatorial coastal station. *Ind J Meteorol and Geophys*, **18**, 497–504.

Prakash Rao, P.S., 1985: Sea breeze at Shar (Revised up to 1984). Indian Space Research Organisation, Tech. Note No. SHAR-05-041-85.

Ramadoss, L.A., 1931: The sea breeze at Karachi. *In* Scientific Notes, Vol. IV. Delhi, India Meteorology Dept.

Ramakrishnan, K.P. and Jambunathan, R., 1958: Sea breeze and maximum temperatures in Madras. *Ind J Meteorol and Geophys*, **9**, 349–358.

Ramanadham, R. and Subbaramayya, I., 1965: The sea breeze at Visakhapatnam. *Ind J Meteorol and Geophys*, **16**, 241–248.

Ramanathan, K.R., 1931: The structure of the sea breeze at Poona. *In* Calcutta, India Meteorology Dept, Scientific Notes, Vol. III.

Rao, D.V., 1955: The speed and some other features of sea-breeze fronts at Madras. *Ind J Meteorol and Geophys*, **6**, 233–242.

Roy, A.K., 1941: The sea breeze at Madras. *In* Scientific Notes, Vol. VIII. Delhi, India Meteorology Dept.

Venkataraman, R. and Prakash Rao, P.S., 1977: Sea breeze at Shar (observed in 1985 and 1986). Indian Space Research Organisation, Tech. Note No. SLEX/PMS/MET/03-002.

UK weather radar picture — 14 January 1989 at 0100 GMT

The United Kingdom weather radar network is now in its tenth year of operation. Fig. 1 shows one of the best examples of the banded nature of precipitation at cold fronts observed since the networks' inception. On this occasion the surface front is marked by line convection elements that extend across the whole network area. The line convection, of the order of 5 km in width (one pixel), is seen at the leading edge of the general area of rain. On the surface chart (Fig. 2), the cold front has been drawn slightly 'stepped' so as to fit the position suggested by radar data. This position is supported by surface observations, a number of which also indicated a temperature drop of 3 to 4 °C, a marked pressure kick and gusts of around 35 kn during frontal passage.

Almost all line convection events occur at 'classical' rearward-sloping cold fronts. The upper-air wind field shown in Fig. 3 is typical of that associated with a classical front with the front lying downstream of a marked jet-entrance region forward of a confluent trough.

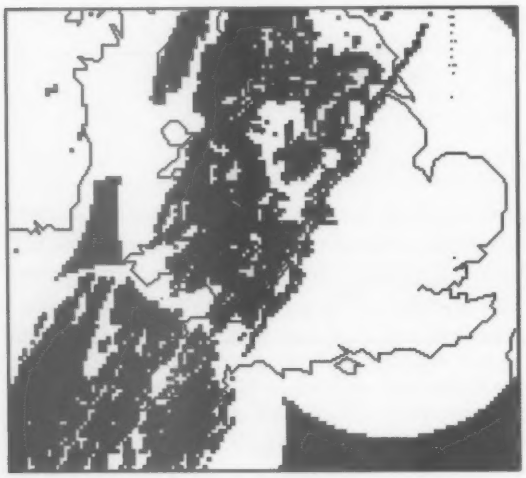

Figure 1. Radar network picture at 0100 GMT 14 January 1989. Rainfall intensities: white 0–½ mm h^{-1}, dark blue ½–1 mm h^{-1}, green 1–4 mm h^{-1}, yellow 4–8 mm h^{-1}, magenta 8–16 mm h^{-1}, red 16–32 mm h^{-1} and cyan > 32 mm h^{-1}.

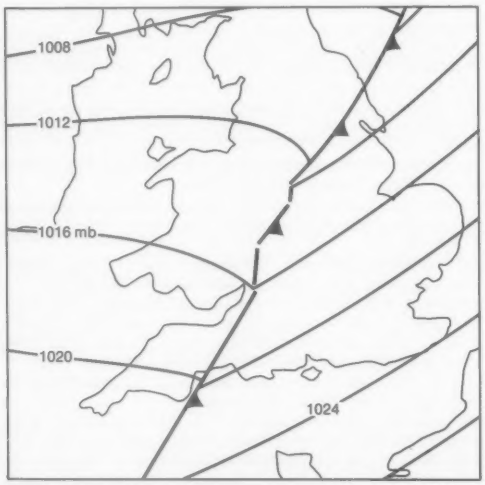

Figure 2. Surface analysis at 0100 GMT 14 January 1989.

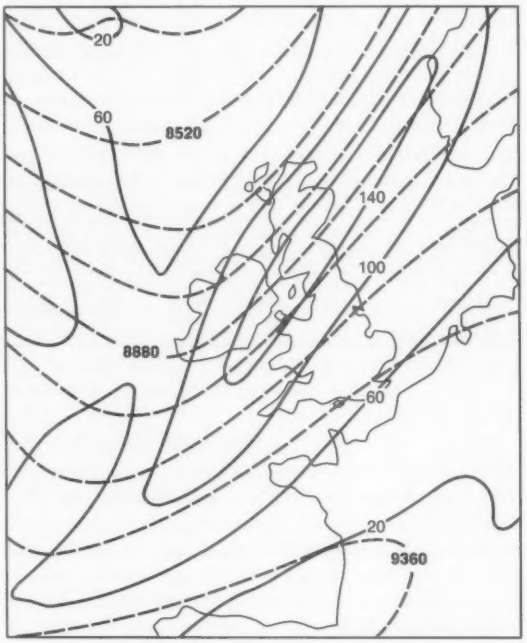

Figure 3. Fine-mesh model-analysed 300 mb isotachs (solid line, contour interval 40 kn) and contours (dashed line, interval 120 m) at 0000 GMT 14 January 1989.

Meteorological Magazine

GUIDE TO AUTHORS

Content

Articles on all aspects of meteorology are welcomed, particularly those which describe the results of research in applied meteorology or the development of practical forecasting techniques.

Preparation and submission of articles

Articles for publication and all other communications for the Editor should be addressed to the Director-General, Meteorological Office, London Road, Bracknell, Berkshire RG12 2SZ and marked 'For *Meteorological Magazine*'.

Articles, which must be in English, should be typed, double-spaced with wide margins, on one side only of A4-size paper. Tables, references and figure captions should be typed separately.

Spelling should conform to the preferred spelling in the *Concise Oxford Dictionary*.

References should be made using the Harvard system (author, date) and full details should be given at the end of the text. If a document referred to is unpublished, details must be given of the library where it may be seen. Documents which are not available to enquirers must not be referred to.

Tables should be numbered using roman numerals and provided with headings. We consider vertical and horizontal rules to be unnecessary in a well-designed table; spaces should be used instead.

Mathematical notation should be written with extreme care. Particular care should be taken to differentiate between Greek letters and Roman letters for which they could be mistaken. Double subscripts and superscripts should be avoided, as they are difficult to typeset and difficult to read. Keep notation as simple as possible; this makes typesetting quicker and therefore cheaper, and reduces the possibility of error. Further guidance is given in BS1991: Part 1: 1976 and *Quantities, Units and Symbols* published by the Royal Society.

Illustrations

Diagrams must be supplied either drawn to professional standards or drawn clearly, preferably in ink. They should be about 1½ to 3 times the final printed size and should not contain any unnecessary or irrelevant details. Any symbols and lettering must be large enough to remain legible after reduction. Explanatory text should not appear on the diagram itself but in the caption. Captions should be typed on a separate sheet of paper and should, as far as possible, explain the meanings of the diagrams without the reader having to refer to the text.

Sharp monochrome photographs on glossy paper are preferred: colour prints are acceptable but the use of colour within the magazine is at the Editor's discretion. In either case contrast should be sufficient to ensure satisfactory reproduction.

Units

SI units, or units approved by WMO, should be used.

Copyright

Authors wishing to retain copyright for themselves or for their sponsors should inform the Editor when they submit contributions which will otherwise become UK Crown copyright by right of first publication.

It is the responsibility of authors to obtain clearance for any copyright material they wish to use before submitting it for publication.

Free copies

Three free copies of the magazine are provided for authors of articles published in it. Separate offprints for each article are not provided.

March 1989

Editor: B.R. May
Editorial Board: R.J. Allam, R. Kershaw, W.H. Moores, P.R.S. Salter

Vol. 118
No. 1400

Contents

Contributions: It is requested that all communications to the Editor and books for review be addressed to the Director-General, Meteorological Office, London Road, Bracknell, Berkshire RG12 2SZ, and marked 'For *Meteorological Magazine*'. Contributors are asked to comply with the guidelines given in the *Guide to authors* which appears on the inside back cover. The responsibility for facts and opinions expressed in the signed articles and letters published in *Meteorological Magazine* rests with their respective authors. Authors wishing to retain copyright for themselves or for their sponsors should inform the Editor when submitting contributions which will otherwise become UK Crown copyright by right of first publication.

Subscriptions: Annual subscription £28.00 including postage; individual copies £2.50 including postage. Applications for postal subscriptions should be made to HMSO, PO Box 276, London SW8 5DT; subscription enquiries 01–211 8667.

Back numbers: Full-size reprints of Vols 1–75 (1866–1940) are available from Johnson Reprint Co. Ltd, 24–28 Oval Road, London NW1 7DX. Complete volumes of *Meteorological Magazine* commencing with volume 54 are available on microfilm from University Microfilms International, 18 Bedford Row, London WC1R 4EJ. Information on microfiche issues is available from Kraus Microfiche, Rte 100, Milwood, NY 10546, USA.

ISBN 0 11 728476 9

ISSN 0026–1149